La mer 23: 158-164, 1985
Société franco-japonaise d'océanographie, Tokyo

Comparison of Lagrangian and Eulerian diffusion near the bottom*

Takashi ICHIYE** and Shoichiro NAKAMOTO**

Abstract: About 360,000 barrels of brine per day were discharged from a diffuser at 22 m deep 20 km south of Freeport, Texas, during 1980 and 1981. Salinity plumes near the diffuser were measured once a month with a towed sled equipped with a sensor fixed 0.8 m high from the bottom. Currents near the diffuser were measured with moored current meters continuously once every four minutes. On nine occasions of plume monitoring the moments of the salinity profiles lateral to the mean current are computed at three distances from the diffuser for each plume. The skewness and kurtosis of the salinity profiles seem to indicate the Gaussian distribution of the profiles. The lateral diffusivity is determined by comparing the second moments with a theoretical solution of the Fickian diffusion equation. The Eulerian correlation function is determined from the current data collected during the period of plume monitoring. The ratio of the Lagrangian to the Eulerian integral time scale is determined by comparing the Lagrangian and Eulerian eddy diffusivity. The Lagrangian time scale is larger in general, but more variable than the Eulerian one. Truncation of the integration limits for calculating moments from salinity profiles reduces estimated values of kurtosis and standard deviation (nominal width of the plume) from the theoretical values obtained for the Gaussian distribution.

1. Introduction

Diffusion in the ocean has been studied for decades in relation to pollution problems. Field experiments were carried out by using dye or drifters in the upper layer of the ocean. This is essentially a Lagrangian approach which provides data related to diffusion processes. However, the Lagrangian type field experiments are difficult to carry out for a long period of time. Further data process and analysis are intricate and the procedures are not well established.

On the other hand, in recent years many projects have been launched to measure currents with moored current meter arrays, particularly in shallow waters for monitering environmental problems in various parts of the world. These programs were mainly devoted to determine currents of tidal and infratidal frequencies. Current spectra in the shallow waters contain substantial energy between the inertial-tidal frequencies and the surface wave frequencies (ICHIYE & TSUJI, 1984). Therefore, the diffusion of pollutants, temperature, salinity or nutrients depends on turbulence of such frequency ranges. However, there is no definite theory which rationalizes relationships between Eulerian correlation function (CF) or spectra with Lagrangian equivalents, though a number of attempts were made to determine such relationships (LUMLEY, 1962; CORRSIN, 1963; KRAICHNAN, 1964) in the inertial subrange.

In order to determine the relationships between Lagrangian and Eulerian CFs, some experiments were carried out in the atmospheric boundary layer (HAY and PASQUILL, 1959; HANNA, 1980). These measurements were for a high frequency range between 10^{-3} sec^{-1} and 1 sec^{-1}, where the ocean turbulence contains relatively low energy. Further, these data did not seem to provide universally applicable relationships, though some speculation of such relationships was applied by OKUBO et al. (1983) in order to explain dye diffusion data and current data collected with moored current meters. There is an urgent need for conclusive oceanic experiments.

The results discussed here are of preliminary nature, since the data were not collected for the

* Received April 2, 1985
** Department of Oceanography, Texas A&M University, College Station, Texas 77843, USA

specific purpose of comparing the Lagrangian diffusion with Eulerian current measurements. However, it shows some direction for future study.

2. Data source

The Strategic Petroleum Reserve Program of the U.S. Department of Energy has discharged brine from a diffuser at the bottom of 22 m deep water about 20 km south of Freeport, Texas, almost continuously at a rate of 360,000 barrels a day since 1980. Currents were measured with a moored current meter array near the diffuser and other hydrographic data were collected by a group of Texas A&M University researchers. Once a month horizontal and vertical distributions of salinity were measured with a salinity sensor attached to a sled which was towed by a small boat (RANDALL et al., 1981).

The horizontal salinity distribution was determined at a height of 0.8 m from the bottom with this sensor within about 8 to 10 hours. An example of the salinity concentration above the ambient salinity is plotted in Fig. 1 with location of sampling stations.

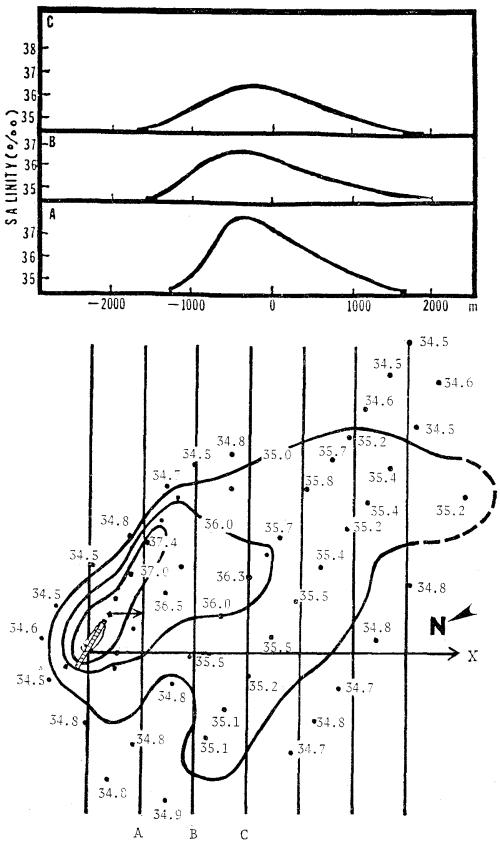

Fig. 1. Salinity contours of a brine plume on August 26, 1980 (Run 3). Brine pit salinity is 216 ‰ and bottom ambient salinity is 34.4 ‰. The direction of the bottom current (speed 27 cms^{-1}) is shown with the arrow in the direction of the x-axis. The distance between transverse sections is 488 m (Randall, 1983; lower panel). The transverse profiles are shown in the upper panel at three distances (488 m, 976 m and 1464 m).

3. Diffusion of brine

Since the brine plume is much larger than the diffuser as indicated in Fig. 1, the source is considered as a point. An approximate solution of Lagrangian diffusion of the brine plume for the continuous point source can be expressed from equation (4.18) of FRENKIEL (1953) in dimensional terms as

$$S(x,y,z)=\frac{Q}{2\pi L_y\bar{v}^2\gamma x}\times\exp\left\{-\frac{U}{4x}\left(\frac{y^2}{L_y\bar{v}^2}+\frac{2z^2}{L_z\bar{w}^2}\right)\right\}, \quad (1)$$

where S is the salinity concentration above the ambient value, Q is the brine discharge rate per unit time, x, y and z axes are parallel to and lateral to the mean flow U, and vertically upwards, respectively, $\bar{u}^2$, $\bar{v}^2$, and $\bar{w}^2$ are mean squares of x-, y- and z-components of turbulent velocity, respectively. Parameters L_x, L_y and L_z represent x-, y- and z-components of the Lagrangian integral scale of turbulence defined by, for instance,

$$L_x=\int_0^\infty R_x(\alpha)d\alpha, \quad (2)$$

with $R_x(\alpha)$ being the Lagrangian CF of turbulent velocity in the x-direction and

$$\gamma^{-2}=(\bar{v}^2L_y/\bar{w}^2L_z), \quad (3)$$

which represents a ratio of vertical to horizontal diffusivity. An impermeable boundary is at $z=0$.

Frenkiel's (1953) model was derived for the isotropic turbulence $L_x=L_y=L_z$ and $\bar{u}^2=\bar{v}^2=\bar{w}^2$. His approximate solution (4.18) was obtained by neglecting the effect of the longitudinal turbulent

velocity $(\bar{u}^2)^{1/2}$ against the advective effect of U.

Solution (1) can be compared to the solution of the Fickian equation of diffusion

$$U\frac{\partial S}{\partial x} = K_y\frac{\partial^2 S}{\partial y^2}+K_z\frac{\partial^2 S}{\partial z^2}, \qquad (4)$$

which yields a solution for a point source at the origin with the impermeable boundary at $z=0$ as

$$S(x, y, z)=\frac{Q}{2\pi(K_yK_z)^{1/2}x}\cdot \times\exp\left(-\frac{Uy^2}{4K_yx}-\frac{Uz^2}{2K_zx}\right). \qquad (5)$$

Therefore, the eddy diffusivities K_y and K_z in the Fickian equation are expressed with the Lagrangian parameters as

$$K_y=\bar{v}^2L_y,\quad K_z=\bar{w}^2L_z. \qquad (6a), (6b)$$

4. Horizontal diffusion of brine

As shown in Fig. 1, salinity distributions at about 0.8 m from the bottom were determined every month from April 1980 through March 1981. During salinity sampling, currents were measured with a moored current array near the diffuser at four depths (3.7 m and 77 m below the surface and 0.5 m and 7.8 m above the bottom). The current meter at 7.8 m yielded most consistent data during the salinity monitoring and thus these data are utilized for this study.

For each salinity sampling the mean current is determined from the current data and x- and y-axes are taken parallel to and perpendicular to the mean current, respectively. The salinity profiles along the y-axis are determined at three distances from the source as shown in Fig. 1. The theoretical distribution along the y-axis are

Table 1. Moments of salinity concentration profiles across a brine plume.

Run #	Date	x (m)	t (hrs)	m_0 (ppt)	m_2 (m^2)	r_3	r_4
#1	4/10/80	244	.5	58.1	17×10^5	6×10^{-3}	2.39
		488	1.04	57.5	18×10^5	2×10^{-5}	2.39
		732	1.56	47.9	11×15^5	2×10^{-3}	2.68
#2	8/1/80	488	3.39	25.05	81×10^4	2×10^{-6}	2.33
		976	6.78	23.15	95×10^4	2×10^{-3}	2.36
		1464	10.17	16.35	70×10^4	5×10^4	2.37
#3	8/26/80	488	.50	31.55	39×10^4	.19	2.59
		976	1.00	27.3	53×10^4	.26	2.48
		1464	1.51	25.6	49×10^4	.03	2.55
#4	10/1/80	244	.85	87.9	84×10^4	1×10^{-3}	2.57
		732	2.54	77.2	90×10^4	.03	2.997
		1464	5.08	64.2	99×10^4	.02	3.00
#5	10/22/80	244	.45	32.9	64×10^4	.01	2.34
		732	1.36	23.7	54×10^4	1×10^{-2}	2.42
		976	1.81	25.2	60×10^4	7×10^{-4}	2.34
#6	12/29/80	244	.48	53.2	12×10^5	.17	2.60
		732	1.45	55.5	17×10^5	.34	2.76
		2196	4.35	41.1	16×10^5	.02	2.43
#7	1/28/81	732	2.5	59.9	16×10^5	.017	2.44
		1464	5.1	64.1	21×10^5	8×10^{-4}	2.26
		2196	7.6	50.8	19×10^5	.068	2.48
#8	2/25/81	244	.97	93.2	14×10^6	2×10^{-4}	2.12
		732	2.90	78.5	14×10^5	8×10^{-3}	3.24
		1464	5.81	55.1	15×10^5	.14	2.45
#9	3/31/81	244	.42	38.6	77×10^3	.288	2.67
		499	.84	36.4	81×10^3	.299	2.73
		732	1.27	26.1	69×10^3	7×10^{-3}	2.52

x : distance from the source
t : x/U (U, mean speed)
m_0: the mean concentration across the profile
m_2: the second moment or nominal width squared
r_3 : skewness
r_4 : kurtosis

determined from the relations

$$m_0=\int_{-\infty}^{\infty} S dy\,, \quad m_1=\int_{-\infty}^{\infty} yS dy\,, \quad (7)$$

$$m_i=\int_{-\infty}^{\infty} (y-m_1)^i (S/m_0) dy\,, \quad (8)$$

for $i=2$ to 4. Then skewness r_3 and kurtosis r_4 are determined from

$$r_3=m_3 \cdot m_2^{-3/2},\ r_4=m_4 \cdot m_2^{-2}\,. \quad (9)$$

In Table 1, m_0, m_2, r_3 and r_4 are listed at three distances from the source for nine runs. The time t is defined as x/U. For the Gaussian profile, $r_3=0$ and $r_4=3$. In general r_3 is small compared to unity and r_4 is close to 3. Skewness shows a degree of deviation of the actual profile from the Gaussian. However, deviation of r_4 from 3 may be partly due to the truncation of the integration limits of the observed profiles (see Appendix).

Significant deviations from the Gaussian distribution were observed within 100 m from the source (not shown), where processes near the diffuser have strong effects on the salinity distribution. ZURBUS and MAMEDOV (1976) also observed a tendency that profiles of dye plumes near the surface become more Gaussian as apart from the source.

The value of m_2 corresponds to the square of the standard deviation σ if the salinity profile along the y-axis is represented by the normalized Gaussian distribution such as

$$f(y)=(\sqrt{2\pi}\sigma)^{-1} \exp\{-y^2/(2\sigma^2)\}. \quad (10)$$

Then 2σ represents a virtual width of the brine plume. Solution (5) averaged with z becomes equivalent to (10) and

$$\sigma=(2K_y x/U)^{1/2}=m_2^{1/2}. \quad (11)$$

(Salinity profiles are almost uniform with height up to 3 m from the bottom.)

Therefore, m_2 should increase linearly with x. However, Table 1 indicates that m_2 is almost constant for each plume. On the other hand, the mean concentration along y is given by

$$\bar{S}=m_0=U^{-1}(\pi x K_y K_z)^{-1/2} \times \exp\{-U_z^2/(4K_z x)\}, \quad (12)$$

if Equation (5) is applicable. This equation indicates that m_0 decreases with x. The values of m_0 determined from the data generally show such a tendency with three exceptions among 18 pairs of profiles. However, since (12) contains an exponential form depending on the vertical eddy diffusivity K_z, K_y cannot be determined from decrease of m_0 with a distance x unless K_z is known. Relation (11) can be used to determine K_y when σ^2 or m_2 is computed from the observed data. Many values of horizontal eddy diffusivity quoted by OKUBO (1972) were obtained in this way.

Determination of m_0 and m_2 depends on truncation of integration limits for the plume, since it is impossible to integrate a salinity profile to infinite values of y. Effects of this truncation on the estimation of σ^2 is also shown in the Appendix. The estimated σ^2 decreases with truncation factor k which is defined as the ratio of an estimated integration limit a to the theoretical σ. The salinity decreases in general as a distance from the source increases. Therefore, the estimated value of the limit a decreases as the distance x increases. Thus, m_2 determined from the data is smaller than the theoretical value of σ^2.

5. Comparison of the Fickian and Lagrangian eddy diffusivity

Equation (6a) shows that the K_y can be determined from the CF of the Lagrangian turbulent velocity v. This velocity can be obtained by use of drifters in the upper ocean layer but it is almost impossible for the bottom boundary layer unless new techniques for tracking the drifters near the bottom are developed. On the other hand, the current near the bottom was monitored within the current meter array as described above. Therefore, if the relationships between the Eulerian and Lagrangian CFs are known, the current meter data can be used for determining K_y.

There is no convincing theory for relationships between the two CFs. HAY and PASQUILL (1959) assumed that the two functions have similarity with different time of t_E and t_L for Eulerian and Lagrangian processes and determined the ratio t_L/t_E as 4 from experiments using pollen dispersion in the atmospheric boundary layer.

Table 2. Comparison of the Fickian and Lagrangian diffusivity.

Run #	Date	U cm s^{-1}	$\overline{v}^2$ cm^{2}s^{-2}	K_f at a distance of 244 m	488 m	732 m m^{2}s^{-1}	976 m	1465 m	2196 m	T_E 10^3s	n mean	S.D.
1	4/10/80	.13	4.26	458.02	234.08	100.81				1.66	357	199
2	8/1/80	.04	3.84		33.21		19.57	9.67		3.46	16	7
3	8/26/80	.27	7.13		106.62		79.40	45.43		4.32	25	8
4	10/1/80	.08	2.33	136.99		49.03		27.12		2.62	117	78
5	10/22/80	.15	7.08	198.18		55.60	46.30			3.45	41	28
6	12/29/80	.14	7.40	340.55		167.21			51.52	3.46	73	46
7	1/28/81	.08	2.24			86.03		56.31	34.03	2.59	101	37
8	2/25/81	.07	2.73	203.66		67.54		34.99		4.32	87	64
9	3/81/81	.16	9.93	25.38	13.35	7.54				5.19	3	1

U : mean speed, n : ratio of the Lagrangian to Eulerian time for correlation function,
$\overline{v^2}$: mean square turbulent velocity, SD: standard deviation.
T_E: Eulerian integral time scale,

TSUJI (1978) confirmed this estimation by comparing the current determined with a drifter and a current meter for several hours in the surface layer of the coastal water of Seto Inland Sea. When the two CFs have similarity with different time related by $t_L=n\,t_E$, then the Lagrangian integral scale of the turbulence L_y can be estimated from the Eulerian correlation function $R_E(t_E)$ as

$$L_y=\int_0^\infty R_L(t_L)dt_L=n\int_0^\infty R_E(t_E)dt_E. \quad (13)$$

The $R_E(t_E)$ is determined by use of the current meter data sampled every 4 minutes at 1.8 m above the bottom. The calculation of R_E is based on a method of DAVIS (1976) and the averaging time of the data is taken from 9 a.m. to 9 p.m. of each salinity monitoring which was carried out only during the daytime. Therefore, calculation used 180 data points. The eddy diffusivity K_y calculated by Equation (11) from m_2 determined by salinity profiles is listed as K_f in Table 2 which also includes $\overline{v}^2$ and $T_E=\int_0^\infty R_E(t_E)dt_E$ with the time interval of 12 hours. Then n can be determined from the formula

$$n=K_f(\overline{v}^2T_E)^{-1}. \quad (14)$$

Since K_f has different values at different distances from the source, the mean value and its standard deviation are determined from each plume and listed also in Table 2.

6. Discussion

Values of n listed in Table 2 are much larger than 4 except for Run 9. Therefore, contention of HAY and PASQUILL (1959) and TSUJI (1976) is not verified. In fact, n is much larger than unity. Since $\overline{v}^2$ is within a range of 2 to 10 cm^2 s^{-2}, and the Eulerian integral time scale T_E $(=L_y)$ within 2×10^3 to 5×10^3 s, Lagrangian time scale T_L must be much larger and is more variable than T_E. These facts indicate that the particle can in general preserve its identity much longer than the current measurements at a fixed station or the Eulerian CFs suggest, but the duration time of such preservation varies more widely than that determined by Eulerian measurements.

An example of the Eulerian CF determined by use of the current meter data of Run 5 is plotted against $h(=t_E/T_E)$ in Fig. 2. An expression which is determined by curve fitting is given by

$$R(h)=\exp\left\{\frac{-h}{b(m^2+1)}\right\}\cos\left(\frac{bh}{m^2+1}\right). \quad (15)$$

This expression was derived theoretically under the assumption of the Markov process of diffusion for a periodic current (FRENKIEL, 1953; ICHIYE and CARNES, 1981). The theoretical equation has $b=1$, whereas the curve fitting yields $b=1.1$. Therefore, the Eulerian CF for the tidal current seems to be expressed by a universal relationship.

The above argument is based on the assumption that the Lagrangian and Eulerian CFs have

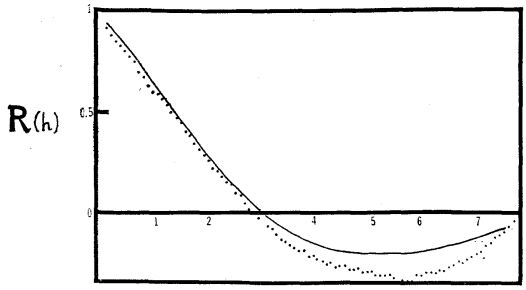

Fig, 2. Eulerian correlation function with $h=t_E/T_E$. Dotted line: from Run 5 (October 22, 1980). Full line: theoretical curve of Equation (14) with $b=1.1$, $m=1.5$.

similarity. This might be valid because CF determined from the current meter data can be approximately expressed with a universal formula. However, this should be verified both by more rigorous mathematical derivation and with field experiments consisting of simultaneous current measurements with the Eulerian and Lagrangian methods, that is, with moored current meters and with drifter tracking. Computer modeling can be used for tracking particles released in the prescribed current fields which nave mean currents and random components with known spectral features. Such modeling will fill the gap of the analytical method and the experimental results.

Appendix. Effects of truncation in concentration profiles

To compute the moments of a concentration distribution S along the y-axis from (7) and (8), the integration limits can not be extended to infinity but must be truncated. This truncation may cause kurtosis different from the theoretical value of 3 even if the distribution is exactly Gaussian as given by (10). On the other hand, the skewness estimated by use of the observed profiles represents deviations from the Gaussian. The effect of truncation on kurtosis can be estimated for the Gaussian distribution by introducing the truncated integrals μ_2 and μ_4 for m_2 and m_4, respectively, where

$$\mu_i=\int_{-k\sigma}^{k\sigma} f(y)\cdot(y-\mu_1)^i dy. \qquad (A.1)$$

The kurtosis determined from the truncated integrals is defined as r_4' which can be expressed as

$$r_4'=\mu_4\cdot\mu_2^3=3\{\mathrm{erf}\,(k/\sqrt{2})-\sqrt{2\pi}/3)k^3 \times(3+k^2)\exp(-k^2/2)\}\cdot\{\mathrm{erf}(k/\sqrt{2}) -\sqrt{2/\pi}\,k\exp(-k^2/2)\}^{-2}, \qquad (A.2)$$

by introducing (10) for $f(y)$ and using the definition of the error function (erf), after the integration limits are taken as $y=\pm k\sigma$. For $k=1$ to 5 the values of r_4' are as follows:

$k=1$	2	3	4	5
$r_4'=0.462$	2.469	2.836	2.986	2.9997

Therefore, the truncation effect may be negligible if the limits are taken 3 times the nominal width of the plume or standard deviation of the concentration σ.

The standard deviation σ estimated from the observed concentration profile also is modified by the truncation. Again, for the Gaussian distribution the estimation of σ can be obtained from the observed distribution as

$$\mu_2/\mu_0=\int_0^{k\sigma} f(y)(y-\mu_1)^2dy\left(\int_0^{k\sigma} f(y)dy\right)^{-1}. \qquad (A.3)$$

By introducing (10) for $f(y)$, this ratio yields

$$\mu_2/\mu_0=\sigma^2N=\sigma^2\{1-\sqrt{2/\pi}\,k \times\exp(-k^2/2)\,\mathrm{erf}\,(k/\sqrt{2})\} \qquad (A.4)$$

instead of σ^2, where N is a correction factor. Values of N for $k=1$ to 4 are as follows:

k	1	1.5	2	2.5	3	3.5	4
N	0.291	0.552	0.774	0.873	0.973	0.994	0.998

This indicates that the truncated integration yields smaller values than σ for the Gaussian distribution. This explains the approximate constancy of σ in the plume at different distances from the source, since the integration limits become smaller because of lower salinity as the distance from the source increases.

References

CORRSIN, S. (1963): Estimates of the relation between Eulerian and Lagrangian scales in large Reynolds number turbulence. J. Atmos. Sci., **20**, 115-119.

DAVIS, R.E. (1976): Predictability of sea surface temperature and sea level pressure anomalies over the North Pacific Ocean. J. Phys. Oceanogr., **6**, 249-266.

FRENKIEL, F.N. (1953): Turbulent diffusion: Mean concentration distribution in a flow field of homogeneous turbulence. Advances in Applied Mechanics, **3**, 61-107, Academic Press, N.Y.

HANNA, S.R. (1980): Lagrangian and Eulerian time-scale relations in the daytime boundary layer. J. Appl. Meteor., **20**, 242-249.

HAY, J.S. and F. PASQUILL (1959): Diffusion from a continuous source in relation to spectrum and scale of turbulence. Advances in Geophysics, **6**, 345-365, Academic Press, N.Y.

ICHIYE, T. and M. CARNES (1981): Sediment dispersion and other environmental impacts of deep-ocean mining in the Eastern Tropical Pacific Ocean. *Marine Environmental Pollution, 2. Dumping and Mining* (Edited by R.A. GEYER), 475-517, Elsevier Sci. Pub. Co., Amsterdam.

ICHIYE, T. and M. TSUJI (1984): Spectra of currents in a shallow sea. 1. Turbulence aspect. La mer (Tokyo), **22**, 104-114.

KRAICHNAN, R.H. (1964): Relation between Lagrangian and Eulerian correlation times of a turbulent velocity field. Phys. Fluids, **7**, 142-153.

LUMLEY, J.L. (1962): An approach to the Eulerian-Lagrangian problem. J. Math. Phys., **3**, 309-312.

OKUBO, A. (1971): Oceanic diffusion diagram. Deep-Sea Res., **18**, 789-802.

OKUBO, A., H. H. CARTER, R. E. WILSON, B. G. SANDERSON and E.N. PARTCH (1983): A Lagrangian and Eulerian diffusion study in the coastal surface layers. Final Report to U.S. Dept. of Energy. Sp. Rept. 46. Ref. 83-1, Marine Science Research Center, SUNY, Stony Brook, N.Y., 295 pp.

RANDALL, R.D. (1983): Analysis of the discharge plume. Evaluation of Brine Disposal from the Bryan Mound Site of the Strategic Petroleum Reserve Program, Tech. Rept. to Dept. of Energy from TAMU Res. Fdn. 1983-I, 108 pp.

TSUJI, M. (1979): Note on the estimation of the Lagrangian and Eulerian time scale ratio from dye plume and current observations. Bull. Nat. Res. Inst. Pol. & Res., **8**, 1-9.

ZHURBAS. V. M. and R. M. MAMEDOV (1976): Experimental study of the diffusion of dye plumes in the surface layer of the sea. Oceanology (English translation by AGU), **16**, 562-564.

海底近くのラグランジュ流とオイラー流の拡散の比較

市 栄 誉, 中 本 正一郎

要旨: 1980年と1981年に約36万バレルの濃塩水を毎日テキサス州フリーポートの南の沖合約20 kmの所で，深さ 22 m の所の拡散穴から海中に放出した。拡散穴の近くの塩水のプリュームを底から0.8 m 上の高さで塩分計をそり状のものにつけ，毎月一回測った。それと同時に流速を拡散穴近くの繋留流速計で4分毎に連続して測った。その中9回のデータを使い，平均流の方向に直角に拡散穴から3つの距離をとり，塩分の水平分布を求め，それから塩分のモーメントを計算した。スキウネスとクルトーシスはガウス分布に近いことを示している。第2次モーメントから横拡散係数をフイックの式の解と比べて求めた。一方流速計のデータからオイラー流の流れの相関関数を求め，ラグランジュおよびオイラーの積分時間尺度を，それぞれの拡散係数を比べることによって定めると前者が後者よりはるかに大きいが，その変動もまた大きい。モーメントを計算する場合，積分の限界が有限があるため，たとえガウス分布でもクルトシスや標準偏差が理論値より小さくなるのでその差の見積りを行った。